Chemical Engineering Journal 430 (2022) 132850

Contents lists available at ScienceDirect

Chemical Engineering Journal

journal homepage: www.elsevier.com/locate/cej

Enhanced kinetic model identification for gas–solid reactions through Computational Fluid Dynamics

Eva-Maria Wartha [a,*], Felix Birkelbach [b], Markus Bösenhofer [a,c], Michael Harasek [a]

[a] TU Wien, Institute of Chemical, Environmental and Bioscience Engineering, Getreidemarkt 9/166, 1060 Vienna, Austria
[b] TU Wien, Institute for Energy Systems and Thermodynamics, Getreidemarkt 9/BA, 1060 Vienna, Austria
[c] K1-Met GmbH, Area 4 - Simulation and Analyses, Stahlstrasse 14, BG 88, 4020 Linz, Austria

ARTICLE INFO

Keywords:
Kinetic modeling
Gas–solid reactions
Virtual experiment
Enhanced data
Computational Fluid Dynamics

ABSTRACT

Gas–solid reactions often play key roles in chemical engineering applications. To understand and design processes featuring such heterogeneous reactions, kinetic models are crucial. One way to identify kinetic models is via thermal analysis experiments. Even if those experiments are carried out meticulously, there will be some deviation between nominal reaction conditions and the actual reaction conditions directly at the reaction site. For situations, where these deviations are not negligible, we propose a new approach to compute the reaction conditions directly at the sample, based on the experimental data. A key feature of our approach is that no kinetic model is required for the simulation. For this reason, the enhanced data can be used for kinetic model identification. Though, a kinetic modeling method that can process arbitrary data is required, because the enhanced kinetic data will not obey the idealized assumptions of constant temperature or constant heating rate.

To showcase our approach, we applied it to the reaction system CuO/Cu_2O. Kinetic models with nominal and simulated values are derived with the TensorNPK method, showing the influence of the enhanced kinetic data on the identified reaction kinetics.

1. Introduction

Interest in kinetic models is two-fold: On the one hand, kinetic models allow us to predict the reaction rate for given reaction conditions. This information is indispensable for reactor design and operation. On the other hand, they provide us with a frame to interpret kinetic data and to gain insights into the reaction mechanism. Regardless of the model purpose, the starting point is always a kinetic data set that contains reaction rate values at various reaction conditions. The quality of the kinetic data set directly determines the quality of the kinetic model. For this reason, collecting kinetic data is a critical step in the modeling process. From the viewpoint of kinetic modeling there are – generally speaking – two main types of experimental error: Error in the reaction rate values and error in the reaction conditions. In this paper, we will focus on the latter.

The most widely used method for measuring the kinetics of gas–solid reactions is thermal analysis (TA). A sample is exposed to controlled reaction conditions (temperature and partial pressure of the reactant gas) and the reaction progress is measured.

To obtain reliable kinetic data, the reaction conditions in TA devices have to be controlled very precisely. This is challenging for three main reasons: First, there are various other processes occurring simultaneously with the chemical reaction under consideration, which are interfering with the control of the reaction conditions. Typical examples are self-heating/cooling, depletion/accumulation of reactant gas or limited gas diffusion. Second, temperature and partial pressure can usually not be measured directly at the sample. The distance between the sample and the sensor leads to a deviation of the measured value from the actual value at the sample. Third, the reaction conditions may not be the same across the whole sample. These effects are the hardest to quantify. Nevertheless, it has been shown in various studies that these inhomogeneities can significantly affect the measurements [1–3].

Most of these measurement errors can be eliminated or at least minimized by conducting the experiments carefully. To guide researchers in this task and establish a reference of best-practices, the ICTAC [1,4] has published a set of recommendations on how to conduct kinetic experiments. Nevertheless, measurement errors cannot be eliminated completely. The effect of mass transfer limitations in TA devices on kinetic analysis was studied by various authors [5–8]. Also deviations of the measured temperature and the temperature of the sample due to thermal lag or due to self-heating/self-cooling have been observed

* Corresponding author.
E-mail address: eva-maria.wartha@tuwien.ac.at (E.-M. Wartha).

https://doi.org/10.1016/j.cej.2021.132850
Received 15 July 2021; Received in revised form 29 September 2021; Accepted 1 October 2021
Available online 12 October 2021

in many experimental studies [9–12]. When those deviations cannot be eliminated completely by adjusting the experimental procedure, computational methods can help to make kinetic data more precise.

The temperature distribution in a TA device has been studied by several authors [2,13–20] using Computational Fluid Dynamics (CFD). Even though it is commonly assumed that the temperature is uniform in the TA device, all of these studies revealed deviations between the assumed or set – further referred to as nominal – temperature assumption, and the actual temperature at the probe. Additionally, Benedetti et al. [21] showed that the gas consumption of the reaction itself leads to reduced concentrations and partial pressures at the reaction site compared to the nominal values. Despite these numerous detailed studies on non-idealities in a TA device, only one work suggested an approach for dealing with these deviations and for deriving more accurate kinetic models: An et al. [22] used a CFD model of a reacting particle in a drop tube furnace to adjust the kinetic rate devolatilization parameters by an iterative procedure, in which they fitted the computational results to the experimental values.

A feature that all the above studies have in common is that they use a reaction model to incorporate the effect of the reaction in the simulation and compute the temperature distribution in the TA device.

If we wanted to use the simulation results for kinetic model identification, we run into a chicken-and-egg situation: in order to do the CFD simulation, a model for the reaction kinetics is needed — but to get enhanced kinetic data for kinetic model identification, the results of the CFD simulation are needed. In this paper we propose an approach that bypasses the need for a kinetic model in the CFD simulation.

The next section discusses the methods that our study is based on. In Section 3 our virtual experimentation approach is introduced. We describe how the experimental data is fed into the simulation model, and we discuss the expected impact on kinetic models. To demonstrate our approach, we chose a kinetic study of the reaction system Cu_2O/CuO (cuprous oxide/cupric oxide). The experimental setup and the experiments conducted in that study are described in Section 4. There, we also describe in detail the simulation model that we employed to recreate the experiments from the study. In Section 5, we first discuss the simulation results and then compare the kinetic model derived from the enhanced data from the virtual experiment with the kinetic model derived based on nominal values for the reaction conditions. We show that dynamic effects in the TA device can affect the kinetic modeling result despite adhering to quality standards for kinetic experiments.

2. Methods

This paper presents an enhanced kinetic modeling approach. For this novel approach, two established methods are employed: CFD for the virtual experimentation and the TensorNPK method for kinetic model identification. This section discusses the basic principles of these methods.

2.1. Computational fluid dynamics

A finite-volume method is used to model the gas–solid reaction process in the experimental setup. We use the open-source object-oriented library OpenFOAM [23], version 7.

The gas phase is modeled as an Eulerian phase, which is described by the continuity equation Eq. (1) and the momentum equations Eq. (2), where ρ_g is the density, $\mathbf{U}_g$ the velocity, τ_g the deviatoric stress of the gas phase. Additionally, the mass source term S_m resulting from reaction and the momentum source term S_u resulting from interaction with the solid phase are used in the equations.

$$\frac{\partial \rho_g}{\partial t} + \nabla \cdot \left(\rho_g \mathbf{U}_g\right) = S_m \tag{1}$$

$$\frac{\partial \left(\rho_g \mathbf{U}_g\right)}{\partial t} + \nabla \cdot \left(\rho_g \mathbf{U}_g \mathbf{U}_g\right) - \nabla \cdot \left(\tau_g\right) = -\nabla p + \rho_g \mathbf{g} + S_u \tag{2}$$

Besides the continuity and momentum equation, the energy equation Eq. (3) and the species equation Eq. (4) are also needed to describe the multi-component gas flow:

$$\frac{\partial \left(\rho_g \left(h + K\right)\right)}{\partial t} + \nabla \cdot \left(\rho_g \mathbf{U}_g \left(h + K\right)\right) - \nabla \cdot \left(\alpha_{\text{eff}} \nabla h\right) = \nabla p + \rho_g \mathbf{U}_g \cdot \mathbf{g} + S_h \tag{3}$$

$$\frac{\partial \rho_g Y_i}{\partial t} + \nabla \cdot \left(\rho_g \mathbf{U}_g Y_i\right) - \nabla \cdot \left(\frac{\mu_{\text{eff}}}{\text{Sc}} \nabla \left(\rho_g Y_i\right)\right) = S_i \tag{4}$$

where h is the enthalpy, K the kinetic energy, α_{eff} the effective thermal diffusivity, Y_i the mass fraction of species i, μ_{eff} the effective viscosity, Sc the Schmidt number and S_h and S_i the energy and species source terms, respectively.

Eq. (1) to Eq. (4) describe the gas phase. The coupling with the solid phase is realized by the source terms S. To compute the species and heat source term S_i and S_h the reaction kinetics are needed which are usually obtained from a kinetic model. In our new approach, we use the experimental data directly to avoid the need of a kinetic model (see Section 3). The solid phase is described within the Lagrangian framework. The particles are regarded as point centers of mass and Newton's law of motion is used to describe their movement:

$$\frac{\mathrm{d}}{\mathrm{d}t}\left(m_p u_p\right) = F \tag{5}$$

where m_p is the particle mass, u_p is the particle velocity, and F is the sum of the forces acting on the particle.

We use a two way coupling approach, which means the velocity of the Eulerian phase directly impacts the Lagrangian particles and vice versa [24]. For the momentum source term, the drag is calculated according to the Gidaspow model [25].

The coupling of the energy equations is done using the Nusselt correlation developed by Ranz and Marshall [26]:

$$\text{Nu} = 2 + 0.6\,\text{Pr}^{1/3}\text{Re}^{1/2} \tag{6}$$

2.2. Kinetic modeling

For the kinetic modeling in this paper we employed the TensorNPK method [27,28]. It is a data-driven method that is based on the General Kinetic Equation (GKE)

$$\frac{\mathrm{d}\alpha}{\mathrm{d}t} = f(\alpha)\, k(T)\, h(p, p_{\text{eq}}), \tag{7}$$

where $f(\alpha)$ is the effect of the conversion α, $k(T)$ the effect of temperature T and $h(p, p_{\text{eq}})$ the effect of the driving force, usually expressed as a function of the partial pressure p and the equilibrium pressure p_{eq}. The GKE is by far the most commonly applied formula to model gas–solid reactions [4]. Essentially, it is a synthesis of solid-state and homogeneous reaction rate models. $f(\alpha)$ models effects in the solid, $k(T)$ an Arrhenius-like temperature effect and $h(p, p_{\text{eq}})$ concentration and equilibrium effects.

The parameter of the $h(p, p_{\text{eq}})$ term depends on the rate limiting step [29]. In [28] we showed that equilibrium effects in gas–solid reactions are best modeled based on the partial molar Gibbs enthalpy of the reaction $G_z(T, p)$. It is defined as the stoichiometric sum of the chemical potentials of the reacting substances. For simple gas–solid reactions, such as the oxidation of Cu_2O in our use case, the partial molar Gibbs enthalpy can also be expressed as a function of the partial pressure and the equilibrium partial pressure. The partial molar Gibbs enthalpy is the driving force of the chemical reaction. It is zero at the equilibrium and increases with distance from the equilibrium. For the kinetic models in this paper, we use the reduced Gibbs enthalpy as a measure for the equilibrium distance.

$$\Delta^{\text{eq}} = \frac{G_z}{\nu_g RT} = \ln \frac{p}{p_{\text{eq}}} \tag{8}$$

Here, ν_g is the stoichiometric coefficient of the gaseous reactant.

The TensorNPK method extracts the effect of each variable (i.e. conversion, temperature and equilibrium distance) on the reaction rate

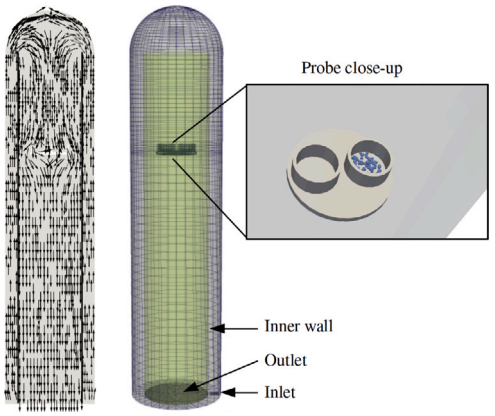

Fig. 1. Flow pattern through the TA device, the mesh and a close-up of the crucible holding the probe (from left to right).

from experimental data. The output of the TensorNPK method are vectors that describe the effect of each variable. These output vectors can be used to predict the reaction rate at given reaction conditions, further analyzed to get more insight into the kinetics or be used to fit reaction models. In this paper, we use the $k(T)$ vector to fit the Arrhenius equation and determine the apparent activation energy E_a. Also, we approximate the $h(\Delta^{eq})$ vector with a second order polynomial to describe the effect.

3. Virtual experiment

Modern thermal analysis (TA) devices use sophisticated strategies to control the reaction conditions as precisely as possible. The sample is placed in a crucible with thin walls made of a material with high thermal conductivity. The temperature sensor measures the temperature directly at the crucible to get a temperature reading as close to the sample as possible. This temperature is controlled to achieve the required temperature profile (isothermal or constant heating rate, usually). Though, the reaction itself will interfere with this temperature control: While the reaction progresses, the heat of reaction has to be compensated by the temperature control. Due to the heat of reaction and thermal lag, the temperature below the crucible can differ from the local temperature in the sample [11].

The reactant partial pressure is usually set by mixing the reactant gas with an inert gas, because most TA devices operate at ambient pressure. The gas flow is controlled with mass flow meters and (ideal) plug flow is assumed. Though, local concentration in the crucible may deviate from the bulk gas flow, because of mixing effects and diffusion effects of the reactant in the inert gas. If the reaction consumes the reactant faster than it can be replenished from the bulk gas flow, the local concentration will drop. Similarly, for reactions that produce gas, reactant gas can accumulate in the crucible.

The experimental procedures have to be carefully designed to reduce or eliminate those deviations. Though, for some reaction systems this might not be possible.

What can be done, when the limits of meticulous experimentation are reached, but the reaction conditions still do not meet the requirements of idealized experimental conditions? For these situations, we propose to couple the experimental analysis with a simulation to quantify the deviations and get accurate estimates of the actual reaction conditions in the sample.

A spatially resolved 3D model of the TGA is generated to recreate the experiment with a CFD simulation — this simulation procedure will be referred to as the virtual experiment. To model the motion of gas and solid phase, and its interaction with the solid reactant, we use established physical CFD models (Section 2.1). When it comes to modeling the reaction, we are confronted with a chicken-and-egg problem: we need a kinetic model for the simulation, but we also need the simulation to derive the kinetic model. This obstacle is overcome by applying the conversion rates obtained from the experiments directly in the simulation. Then, no kinetic model is needed. The measured conversion rates are set as fixed conversion rates in the CFD simulation. The only assumption required is that all particles react uniformly. This is inherently ensured within TA experiments, where uniform reaction progress needs to be ensured by choosing a sufficiently small sample mass [1,30], since the conversion rate is determined by one measurement only.

Regarding kinetic model identification, a caveat of our approach is that the simulated reaction conditions will generally deviate from idealized reaction conditions such as “isothermal” or “constant heating rate”. Consequently, most established kinetic modeling methods cannot be used with the presented approach, because they are based on exactly these idealized assumptions. To take advantage of the simulated reaction conditions from the virtual experiment for kinetic model identification, the kinetic modeling method needs the capability to process arbitrarily distributed data points. The TensorNPK method [27,28] meets these requirements. Another option would have been to use direct model fitting methods [31], but they require an a-priori selection of the model terms, which could conceal important information. For this reason, we chose the data-driven approach with the TensorNPK to process the data from the virtual experiments. The only requirement for the TensorNPK, is that the reaction obeys the GKE.

4. Use case

In general, the proposed approach can be applied to any gas–solid reaction system. To demonstrate the suggested approach and make the effects on kinetic model identification palpable, we use a set of kinetic measurements for the reaction system cuprous oxide/cupric oxide

$$2Cu_2O + O_2 \rightleftarrows 4CuO$$

that were conducted by Setoodeh Jahromy et al. [32]. This reaction system is of interest, because it is a promising candidate for thermochemical energy storage systems [33,34]. The experiments were recreated using OpenFOAM. In this section we will first describe the experimental setup that was used for the measurements, and then we will describe the simulation setup that was used to recreate these measurements.

4.1. Experimental setup

The reaction Cu_2O/CuO was studied via simultaneous TA measurements on a NETZSCH STA 449 C JUPITER. The apparatus has a combined TGA-DSC (thermogravimetric analysis — differential scanning calorimetry) sample holder. For the measurements aluminum oxide crucibles were used. Experiments were conducted at ambient pressure. The total gas flow (N_2 and O_2) was set to 100 mL/min always, using red-y smart series mass-flow controllers by Voegtlin. The reaction was initiated by switching from pure N_2 to a mix of O_2 and N_2. The mixing ratio was adjusted to achieve the studied oxygen partial pressures. The sample temperature was measured right below the crucible and controlled by the TA software.

To rule out inhomogeneous reaction conditions within the probe, the sample mass was adjusted so that no effect on the reaction progress could be observed. A sufficiently small sample mass should ensure that there are no concentration or temperature gradients within the probe; this means that the conversion progress is not influenced by the mass itself. This was experimentally confirmed for the experiments in our use case [32].

The experiments were conducted with a Cu_2O sample mass of 8.26 mg and for a combination of nominal temperatures (800, 830, 880 and 930 °C) and nominal oxygen partial pressures (0.1, 0.2, 0.5 and 1 bar).

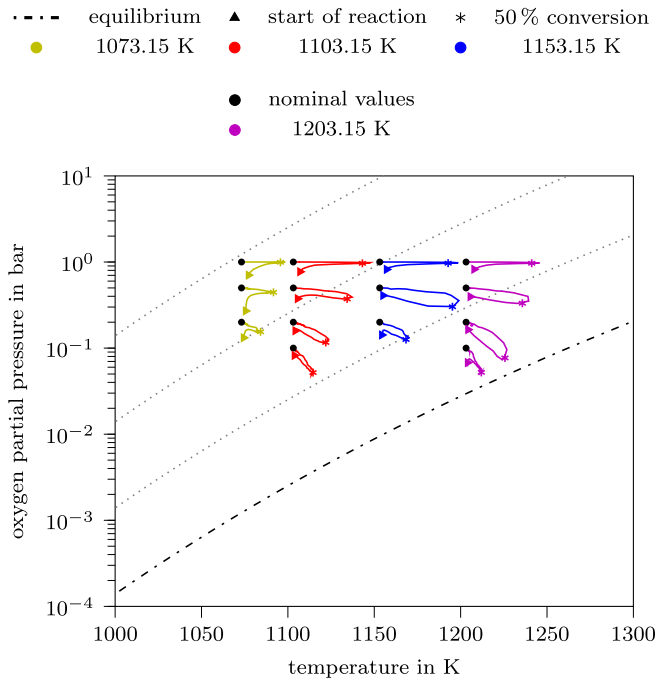

Fig. 2. Temperature and partial pressure at the probe. Nominal values (black dots) and simulated trajectories (in color — color-coded with the nominal temperature). Reaction equilibrium (dash-dotted) and equidistant lines (dotted) are marked.

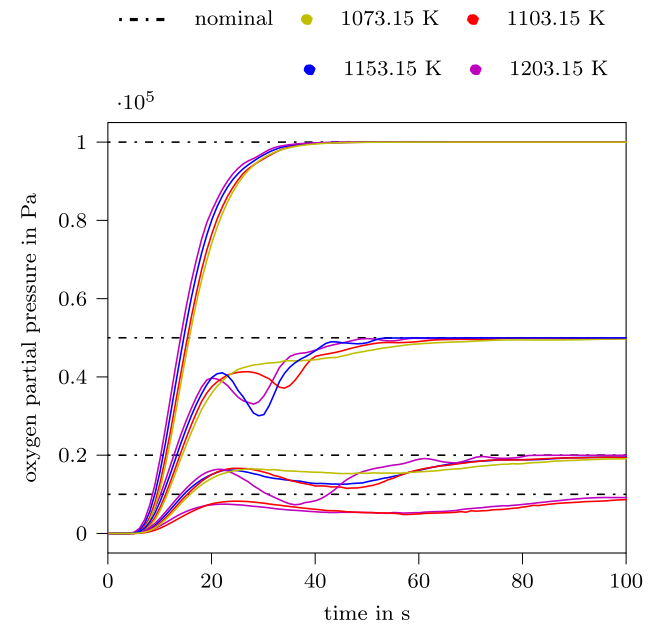

Fig. 3. Comparison between the nominal partial pressure and the actual partial pressure at the probe.

4.2. CFD setup

The TA apparatus was discretized with 30 600 hexahedral cells, displayed in Fig. 1. The solid walls were excluded in the simulation, and the wall temperature was fixed to the nominal-temperature, because this is controlled in the TA device. The mass flow and composition at the inlet were fixed according to the experimental setup. The sample was initialized as Cu_2O at the beginning of the experiment. The solid reactant was modeled by 209 Lagrangian parcels, with 10^5 particles per parcel with a particle diameter of 5 μm. The experimental particle size distribution obtained with a Mastersizer 2000 [32] showed a bi-modal distribution. For this reason, the median diameter of the experimental particle size distribution was used.

Table 1
Thermodynamic properties of the solid reactants.

	W g mol^{-1}	H_f J mol^{-1}	c_p J kg^{-1} K^{-1}	ρ kg m^{-3}	κ W m^{-1} K^{-1}
Cu_2O	143.091	−1 192 248	609	6000	0.78
CuO	79.545	−1 958 639	600	6480	0.78

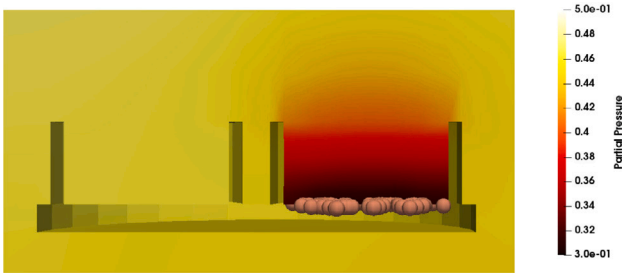

Fig. 4. Oxygen partial pressure of the virtual experiment at 1153.15 K and 0.5 bar oxygen partial pressure (nominal conditions) after 27 s experimental time, at 25 % conversion.

The gas phase is modeled as perfect gas, the viscosity is calculated based on the Sutherland model, with the Sutherland coefficients ($A_s = 1.512e-6$ and $T_s = 120$) from [35]. The heat capacity c_p is calculated from JANAF polynomials from [35], see Table 2.

For the solid species the thermal conductivity κ, density ρ and heat capacity c_p are assumed constant. They are given in Table 1 along with the heat of formation H_f and the molecular weight.

5. Results and discussion

In the previous sections we introduced the virtual experiment and explained how it is coupled with the real experiment to make use of the enhanced data. Now, we will showcase the method by applying it to the use case of Cu_2O oxidation. First, we discuss the deviations between nominal values and the values from the virtual experiment as well as the causes for these deviations. Then, we examine the effect on the identified kinetic model.

Fig. 2 shows the change of the reaction conditions during the virtual experiment in relation to the nominal values. Even though a very small sample mass has been used in the experiments (8.26 mg), the distance to the equilibrium reduces drastically compared to nominal values due to self-heating of the probe and a drop of the partial pressure. The temperature at the start of the reaction corresponds to the nominal temperature, but during the experiment the temperature increases due to the rapid release of reaction heat that cannot be dissipated instantly. This temperature increase also reduces the distance to equilibrium and consequently the driving force of the reaction. The drop in the oxygen partial pressure also contributes to the reduction of the equilibrium distance.

Fig. 3 shows the oxygen partial pressure in more detail. Initially, the partial pressure is zero, because the TA device is flooded with N_2 before the experiment. When the gas flow is switched to the O_2/N_2 mixture, the partial pressure quickly rises. Though, it does not do so immediately. This deviation from ideal plug-flow can be attributed to back mixing and diffusion. Once the reaction starts, there is an obvious drop in the partial pressure that is caused by the reactant depletion in close vicinity of the sample. Comparing the partial pressure drops in Fig. 3, it can be seen that the drop is more pronounced the faster the reaction proceeds, but in pure O_2 atmosphere, where the reaction is fastest, there is no drop in the partial pressure. This observation

suggests that the drop in partial pressure is caused by limited O_2 diffusion in N_2 atmosphere. This is in accordance with similar findings for gasification processes [36,37].

To visualize the reactant depletion at the sample, we chose the experiment with the nominal values 1153.15 K and 0.5 bar oxygen partial pressure, where the effect of reactant depletion is especially pronounced. Fig. 4 gives a close look on this effect inside the TA device. The partial pressure near the solid reactant is drastically reduced and the partial pressure gradient is clearly visible. Similar effects have been observed by [2,16,17].

The deviations between the idealized assumptions of constant temperature or partial pressure have been studied extensively, for example by [2,15–18]. A central take-away point of our study is, that it is possible to quantify these effects by setting up a CFD simulation and performing a virtual experiment. The results from the virtual experiment can be used to estimate the sample temperature and partial pressure in situations, when it is not feasible to improve the experimental design to the point where unwanted effects are eliminated completely and no deviations between the measured or nominal conditions and the actual conditions at the probe occur. Though, this approach is not meant to replace careful experimentation.

To make the impact on the kinetic model palpable, we used both the nominal values and the simulated values to derive kinetic models for the oxidation of Cu_2O with the TensorNPK method. Fig. 5 shows the contributions of conversion, temperature and distance to equilibrium according to the GKE. The simulated temperature and partial pressure affects the estimation of the $k(T)$ and $h(\Delta^{eq})$ terms in the GKE. With simulated values, the temperature sensitivity is considerably lower than with nominal values. This is, because high reaction rates are attributed to higher temperatures when self-heating is taken into consideration (Fig. 2). A similar observation can be made for the effect of the equilibrium distance: With simulated values it is less steep in close proximity to the equilibrium, because high reaction rates are attributed to smaller distances to the equilibrium.

This larger temperature sensitivity can also be seen in the activation energies that are derived from the $k(T)$ values: With nominal values the apparent activation energy is 218.9 kJ/mol; with simulated values it is 197.5 kJ/mol.

The estimation of the contributions to the GKE and the effect on the fitted models – such as the Arrhenius equation – show a significant impact of self-heating and reactant depletion. If these effects are not taken into account when deriving a kinetic model, this can have a practical meaning for chemical engineering applications. To illustrate this, we plotted the effective temperature dependency in Fig. 6. It shows the predicted reaction rate as a function of temperature at fixed oxygen partial pressures and $\alpha = 0.5$. These curves have been generated with the Arrhenius function and the second order polynomial fit to the effect of the equilibrium distance (solid lines in Fig. 5). Note, that the temperature input values to the kinetic models were in the range from 1070 K to 1200 K. The effective temperature dependency beyond these values is extrapolated. Even though the diagram should not be overinterpreted for this reason, it is a good illustration of the impact of self-heating and reactant depletion on the kinetic model nonetheless.

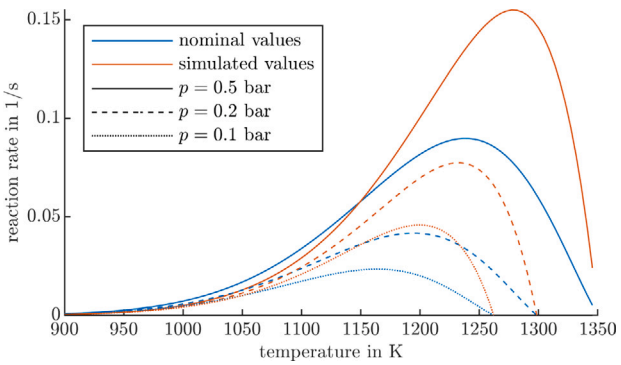

Fig. 6. Effective temperature dependency based on the two kinetic models in Fig. 5. The models were evaluated at $\alpha = 0.5$ and three partial pressures.

Table 2
Coefficients for the heat capacity calculated based on JANAF polynomials taken from [35].

N_2	3.531 01	−0.000 123 661	$-5.029\ 99 \cdot 10^{-7}$	$2.435\ 31 \cdot 10^{-9}$
	$-1.40881 \cdot 10^{-12}$	−1046.98	2.967 47	
O_2	3.782 46	−0.002 996 73	$9.8473 \cdot 10^{-6}$	$-9.6813 \cdot 10^{-9}$
	$3.243\ 73 \cdot 10^{-12}$	−1063.94	3.657 68	

The most striking difference between the two predictions is that the model based on enhanced kinetic data shows a much higher reaction rate peak. In general, the rate is dominated by the exponential Arrhenius function far away from the equilibrium, and then drops sharply towards the equilibrium. Thus, the later the drop, the higher the peak. The position of the drop depends mainly on the steepness at which the equilibrium dependency $h(\Delta^{eq})$ approaches zero. Fig. 5 shows that the model derived from simulated values is much steeper and, thus, it features higher peaks in the effective temperature dependency. The reason for this difference in steepness is, that the simulation showed that the experimental conversion rates need to be attributed to temperatures and partial pressures much closer to the equilibrium than the nominal values suggested.

This change of the peak has practical implications: It means that optimal (in the sense of highest rate) reaction conditions can be achieved much closer to the equilibrium than the nominal model would suggest. In fact, the peak reaction rate can be achieved at about 40 K above the prediction with nominal values. For applications in thermochemical energy storage, for example, this is good news. If the storage material can be operated at higher temperatures, the thermal efficiency can be expected to be considerably higher.

The observations on the CuO/Cu_2O reaction system demonstrated the possible effects of incorporating enhanced data in kinetic model identification, which could be done in the proposed way for any gas–solid reaction system. Although careful experimentation is still indispensable, the suggested approach to couple a virtual experiment with kinetic model identification paves the way towards more precise analysis of gas–solid reactions.

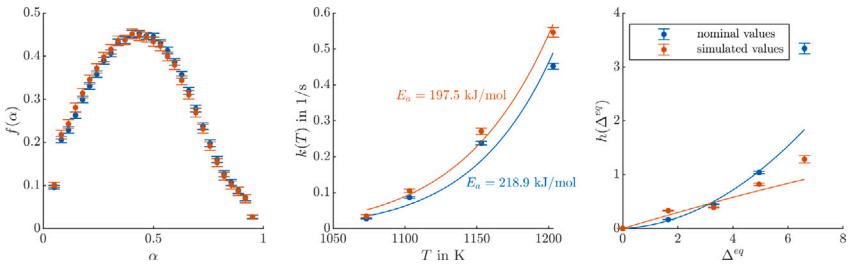

Fig. 5. Output of the TensorNPK method using the nominal reaction conditions and the simulated values as input.

6. Conclusion

Accurate readings of the actual reaction conditions of the sample are essential for deriving reliable kinetic models. Even if experiments are conducted meticulously, nominal temperature and partial pressure values are known to be deviating from the actual conditions at the sample due to effects such as self-heating and reactant depletion.

These effects are inherent to gas–solid reactions and can never be eliminated completely. Though, with the presented method, the deviations can be quantified through a virtual experiment and the kinetic data can be enhanced. In the virtual experiment the temperature and partial pressure at the probe-site are determined with a CFD simulation which also takes into account the effect of the chemical reaction itself. The key novelty of our approach is that no kinetic model is required for the simulation. Instead, the reaction is modeled by using the experimentally determined conversion rates as direct input into the CFD simulation. In this way, the result of the virtual experiment can be used for kinetic model identification.

Since the enhanced data does not necessarily obey any simplified reaction conditions, e.g. isothermal or constant heating rate, a method to process arbitrary data for kinetic model identification is necessary.

To demonstrate our approach, we applied our approach to the oxidation of Cu_2O and used the TensorNPK method to derive two kinetic models: one using the classical approach with nominal values, and one using the reaction conditions directly at the sample calculated in the virtual experiment. The difference in the derived models can be critical for chemical engineering applications such as reactor design.

The results show that virtual experiments are a versatile tool to enhance experimental results when measured values are expected to be affected by effects such as self-heating/cooling and reactant depletion/accumulation. However, it is not meant to replace precise experimentation. Carefully planning, preparing and conducting experiments should still have highest priority. Our approach allows to quantify non-idealities in the virtual experiment and incorporate them in the kinetic model identification.

List of acronyms

CFD	Computational Fluid Dynamics
DSC	Differential Scanning Calorimetry
GKE	General Kinetic Equation
NPK	Non-parametric Kinetics
TA	Thermal Analysis
TGA	Thermogravimetric Analysis

List of symbols

symbol	name	unit
c_p	heat capacity	$J\,kg^{-1}\,K^{-1}$
$\mathbf{g}$	gravitational acceleration	$m\,s^{-2}$
h	enthalpy	$J\,kg^{-1}$
H_f	heat of formation	$J\,kg^{-1}$
K	kinetic energy	$m^2\,s^{-2}$
p	pressure	Pa
S_h	energy source term	$J\,m^{-3}\,s^{-1}$
S_m	mass source term	$kg\,m^{-3}\,s^{-1}$
S_u	momentum source term	$N\,m^{-3}\,s^{-1}$
t	time	s
$\mathbf{U}$	velocity vector	$m\,s^{-1}$
W	molecular weight	$g\,mol^{-1}$
Y_i	mass fraction of species i	$kg\,kg^{-1}$
α_{eff}	effective thermal diffusivity	$m^2\,s^{-1}$
κ	thermal conductivity	$W\,m^{-1}\,K^{-1}$
μ_{eff}	effective viscosity	Pa s
ρ	density	$kg\,m^{-3}$
τ	deviatoric stress tensor	$N\,m^{-2}$

Declaration of competing interest

The authors declare that they have no known competing financial interests or personal relationships that could have appeared to influence the work reported in this paper.

Acknowledgments

The authors gratefully acknowledge the funding support of K1-MET GmbH, Austria, metallurgical competence center. The research program of the competence center K1-MET is supported by COMET (Competence Center for Excellent Technologies), the Austrian program for competence centers. COMET is funded by the Federal Ministry for Transport, Innovation and Technology, the Federal Ministry for Science, Research and Economy, the provinces of Upper Austria, Tyrol, and Styria, and the Styrian Business Promotion Agency. The authors acknowledge TU Wien Bibliothek for financial support through its Open Access Funding Programme.

References

[1] S. Vyazovkin, K. Chrissafis, M.L. Di Lorenzo, N. Koga, M. Pijolat, B. Roduit, N. Sbirrazzuoli, J.J. Suñol, ICTAC kinetics committee recommendations for collecting experimental thermal analysis data for kinetic computations, Thermochimica Acta 590 (2014) 1–23, http://dx.doi.org/10.1016/j.tca.2014.05.036.

[2] S. Schulze, P. Nikrityuk, Z. Abosteif, S. Guhl, A. Richter, B. Meyer, Heat and mass transfer within thermogravimetric analyser: From simulation to improved estimation of kinetic data for char gasification, Fuel 187 (2017) 338–348, http://dx.doi.org/10.1016/j.fuel.2016.09.048.

[3] A. Gomez, N. Mahinpey, Kinetic study of coal steam and CO2 gasification: A new method to reduce interparticle diffusion, Fuel 148 (2015) 160–167, http://dx.doi.org/10.1016/j.fuel.2015.01.071.

[4] S. Vyazovkin, A.K. Burnham, J.M. Criado, L.A. Pérez-Maqueda, C. Popescu, N. Sbirrazzuoli, ICTAC kinetics committee recommendations for performing kinetic computations on thermal analysis data, Thermochimica Acta 520 (2011) 1–19, http://dx.doi.org/10.1016/j.tca.2011.03.034.

[5] B. Nowak, O. Karlström, P. Backman, A. Brink, M. Zevenhoven, S. Voglsam, F. Winter, M. Hupa, Mass transfer limitation in thermogravimetry of biomass gasification, J. Therm. Anal. Calorim. 111 (1) (2013) 183–192, http://dx.doi.org/10.1007/s10973-012-2400-9.

[6] A. Jess, A.K. Andresen, Influence of mass transfer on thermogravimetric analysis of combustion and gasification reactivity of coke, Fuel 89 (7) (2010) 1541–1548, http://dx.doi.org/10.1016/j.fuel.2009.09.002.

[7] P. Geng, Y. Zhang, Y. Zheng, Experimental estimate of CO2 concentration distribution in the stagnant gas layer inside the thermogravimetric analysis (TGA) crucible, Fuel 224 (2018) 250–254, http://dx.doi.org/10.1016/j.fuel.2018.03.057.

[8] M. Malekshahian, A. De Visscher, J.M. Hill, A non-equimolar mass transfer model for carbon dioxide gasification studies by thermogravimetric analysis, Fuel Process. Technol. 124 (2014) 1–10, http://dx.doi.org/10.1016/j.fuproc.2014.02.009.

[9] R. Narayan, M.J. Antal, Thermal lag, fusion, and the compensation effect during biomass pyrolysis, Ind. Eng. Chem. Res. 35 (5) (1996) 1711–1721, http://dx.doi.org/10.1021/ie950368i.

[10] M.J. Antal, G. Várhegyi, Impact of systematic errors on the determination of cellulose pyrolysis kinetics, Energy Fuels 11 (6) (1997) 1309–1310, http://dx.doi.org/10.1021/ef970030w.

[11] O. Vekemans, J.P. Laviolette, J. Chaouki, Thermal behavior of an engineered fuel and its constituents for a large range of heating rates with emphasis on heat transfer limitations, Thermochim. Acta 601 (2015) 54–62, http://dx.doi.org/10.1016/j.tca.2014.12.007.

[12] C. Branca, C. Di Blasi, Self-heating effects in the thermogravimetric analysis of wood char oxidation, Fuel 276 (April) (2020) 118012, http://dx.doi.org/10.1016/j.fuel.2020.118012.

[13] R. Comesaña, Contribuciones al modelado CFD de la Pirólisis de Biomassa Sólida Mediante la Simulación, Mejora y contraste experimental de un TG-FTIR, (Thesis doctoral), Universidade de Vigo, 2011.

[14] R. Comesaña, M.A. Gómez, M.A. Àlvarez, P. Eguía, Thermal lag analysis on a simulated TGA-DSC device, Thermochim. Acta 547 (2012) 13–21, http://dx.doi.org/10.1016/j.tca.2012.08.008.

[15] R. Comesaña, M.A. Gómez, M.A.A. Feijoo, P. Eguía, CFD simulation of a TG – DSC furnace during the indium phase change process, Appl. Energy 102 (2013) 293–298, http://dx.doi.org/10.1016/j.apenergy.2012.07.019.

[16] R. Buczyński, G. Czerski, K. Zubek, R. Weber, P. Grzywacz, Evaluation of carbon dioxide gasification kinetics on the basis of non–isothermal measurements and CFD modelling of the thermogravimetric analyser, Fuel 228 (2018) 50–61, http://dx.doi.org/10.1016/j.fuel.2018.04.134.

[17] S. Lan, M. Gaeini, H. Zondag, A.V. Steenhoven, C. Rindt, Direct numerical simulation of the thermal dehydration reaction in a TGA experiment, Appl. Therm. Eng. 128 (2018) 1175–1185, http://dx.doi.org/10.1016/j.applthermaleng.2017.08.073.

[18] D. De La Cuesta, M.A. Gómez, J. Portteiro, L. Febrero, E. Granada, E. Arce, CFD analysis of a TG – DSC apparatus, J. Therm. Anal. Calorim. 118 (2014) 641–650, http://dx.doi.org/10.1007/s10973-014-3734-2.

[19] L. Favergeon, J. Morandini, M. Pijolat, M. Soustelle, A general approach for kinetic modeling of solid-gas reactions at reactor scale : Application to kaolinite dehydroxylation, Oil Gas Sci. Technol. Rev. IFP Energies Nouvelles 68 (6) (2013) 1039–1048, http://dx.doi.org/10.2516/ogst/2012018.

[20] V. Furtado de Moura, Análise térmica computacional via cfd openfoam, (Doctoral thesis), Universidade Federal do Espírito Santo, 2018.

[21] A. Benedetti, M. Modesti, M. Strumendo, Cfd analysis of the CaO-CO_2 reaction in a thermo- gravimetric apparatus, Chem. Eng. Trans. 43 (2015) 1039–1044, http://dx.doi.org/10.3303/CET1543174.

[22] F. An, F. Küster, R. Ackermann, S. Guhl, A. Richter, Heat and mass transfer analysis of a high-pressure TGA with defined gas flow for single-particle studies, Chem. Eng. J. 411 (January) (2021) 128503, http://dx.doi.org/10.1016/j.cej.2021.128503.

[23] H. Weller, G. Tabor, H. Jasak, C. Fureby, A tensorial approach to computational continuum mechanics using object-oriented techniques, Comput. Phys. 12 (6) (1998) 620–631, http://dx.doi.org/10.1063/1.168744.

[24] H.A. Jakobsen, Chemical Reactor Modeling : Multiphase Reactive Flows, Springer, Berlin [u.a.], 2008.

[25] D. Gidaspow, Multiphase Flow and Fluidization. – Continuum and Kinetic Theory Descriptions, Academic Press Inc., 1994.

[26] W.E. Ranz, W.R.J. Marshall, Evaporation from drops Part I, Chem. Eng. Progress 48 (3) (1952) 141–146.

[27] F. Birkelbach, M. Deutsch, S. Flegkas, F. Winter, A. Werner, NPK 2.0: Introducing tensor decompositions to the kinetic analysis of gas-solid reactions, Int. J. Chem. Kinetics 51 (4) (2019) 280–290, http://dx.doi.org/10.1002/kin.21251.

[28] F. Birkelbach, M. Deutsch, A. Werner, The effect of the reaction equilibrium on the kinetics of gas-solid reactions — A non-parametric modeling study, Renew. Energy 152 (2020) 300–307, http://dx.doi.org/10.1016/j.renene.2020.01.033.

[29] L.-C. Söğütoğlu, F. Birkelbach, A. Werner, H. Fischer, H. Huinink, O. Adan, Hydration of salts as a two-step process: Water adsorption and hydrate formation, Thermochim. Acta 695 (2021) 178819, http://dx.doi.org/10.1016/j.tca.2020.178819.

[30] N. Saadatkhah, A. Carillo Garcia, S. Ackermann, P. Leclerc, M. Latifi, S. Samih, G.S. Patience, J. Chaouki, Experimental methods in chemical engineering: Thermogravimetric analysis—TGA, Canadian J. Chem. Eng. 98 (1) (2020) 34–43, http://dx.doi.org/10.1002/cjce.23673.

[31] J. Opfermann, Kinetic analysis using multivariate non-linear regression. I. Basic concepts, J. Therm. Anal. Calorim. 60 (2) (2000) 641–658, http://dx.doi.org/10.1023/A:1010167626551.

[32] S. Setoodeh Jahromy, F. Birkelbach, C. Jordan, C. Huber, M. Harasek, A. Werner, F. Winter, Impact of partial pressure, conversion, and temperature on the oxidation reaction kinetics of Cu_2O to CuO in thermochemical energy storage, Energies 12 (3) (2019) 508, http://dx.doi.org/10.3390/en12030508.

[33] M. Deutsch, F. Horvath, C. Knoll, D. Lager, C. Gierl-Mayer, P. Weinberger, F. Winter, High-temperature energy storage: Kinetic investigations of the CuO/Cu2O reaction cycle, Energy Fuels 31 (3) (2017) 2324–2334, http://dx.doi.org/10.1021/acs.energyfuels.6b02343.

[34] E. Alonso, C. Pérez-Rábago, J. Licurgo, E. Fuentealba, C.A. Estrada, First experimental studies of solar redox reactions of copper oxides for thermochemical energy storage, Sol. Energy 115 (2015) 297–305, http://dx.doi.org/10.1016/j.solener.2015.03.005.

[35] G.P. Smith, D.M. Golden, M. Frenklach, N.W. Moriarty, B. Eiteneer, M. Goldenberg, C.T. Bowman, R.K. Hanson, S. Song, W.C.J. Gardiner, V.V. Lissianski, Z. Qin, GRI-MECH 3.0, 2017, URL http://www.me.berkeley.edu/gri-mech/.

[36] Y. Zhang, P. Geng, Y. Zheng, Exploration and practice to improve the kinetic analysis of char-CO2 gasification via thermogravimetric analysis, Chem. Eng. J. 359 (2019) 298–304, http://dx.doi.org/10.1016/j.cej.2018.11.122.

[37] A. Gómez-Barea, P. Ollero, R. Arjona, Reaction-diffusion model of TGA gasification experiments for estimating diffusional effects, Fuel 84 (12–13) (2005) 1695–1704, http://dx.doi.org/10.1016/j.fuel.2005.02.003.